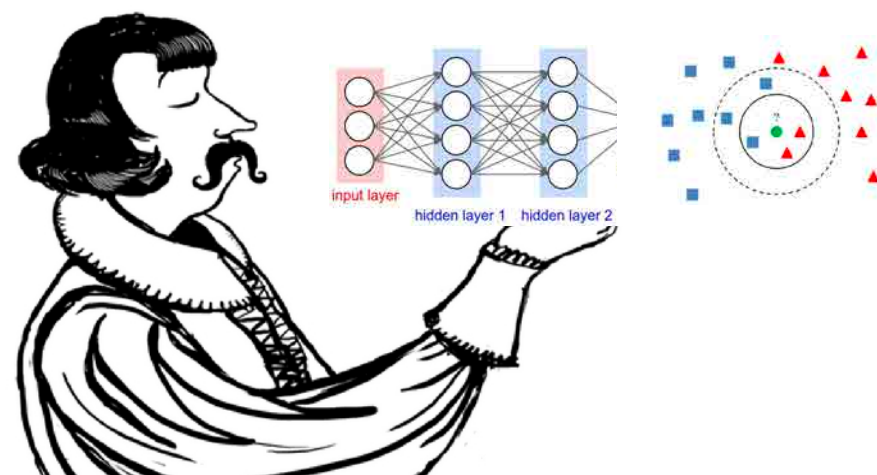

The Need for Geometric Regularization: Theory and Examples in Image Classification and Face/Person Challenges

Guillermo Sapiro
Duke University

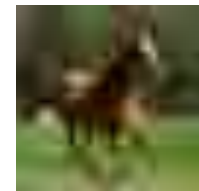
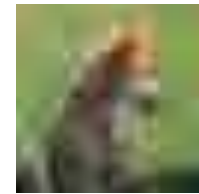
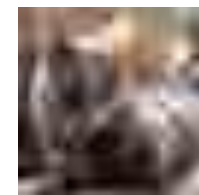
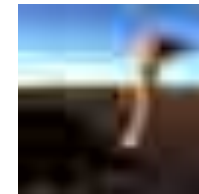
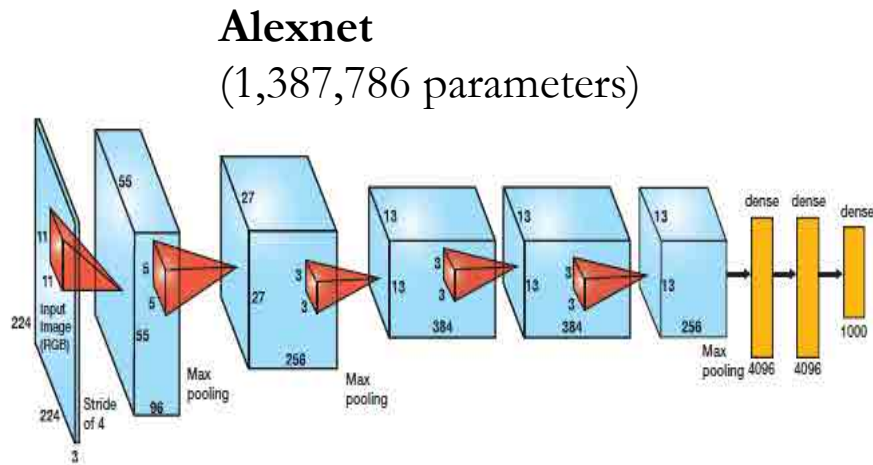
DNN or kNN: That is the Generalize vs Memorize Question

Guillermo Sapiro
Duke University

With Gilad Cohen and Raja Giryes



Object Recognition using Deep Learning



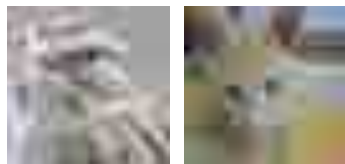
Train accuracy: 99.90%

Test accuracy: 81.22%

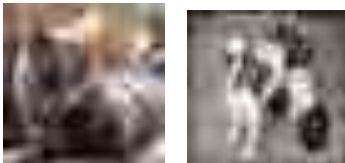
Object Recognition using Deep Learning



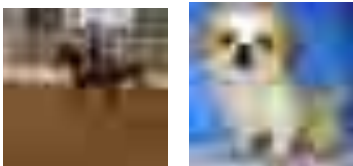
bird horse



airplane dog

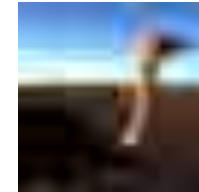
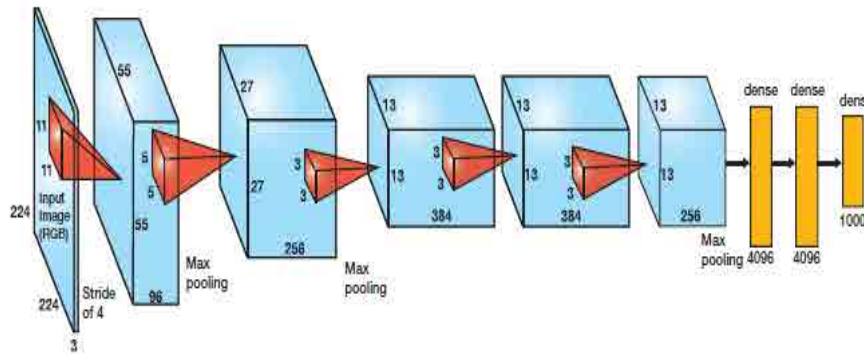


bird cat

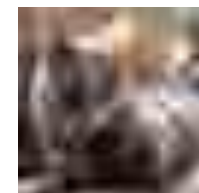


dog airplane

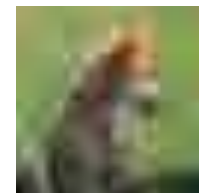
Alexnet
(1,387,786 parameters)



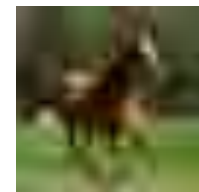
← ?



← ?



← ?

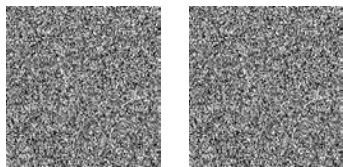


← ?

Train accuracy: 99.82%

Test accuracy: 9.86%

Object Recognition using Deep Learning

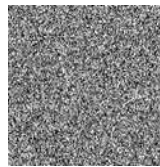


bird

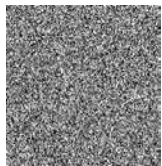
horse



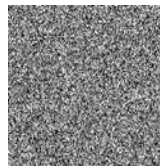
airplane



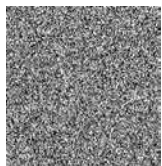
dog



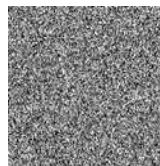
bird



cat



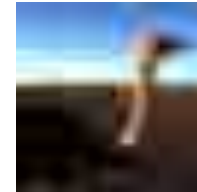
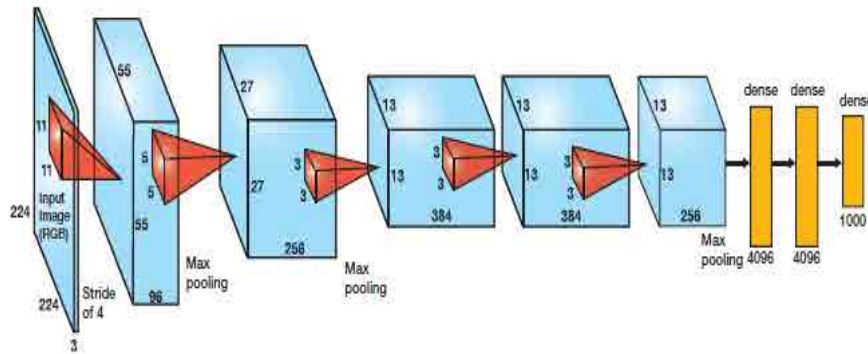
dog



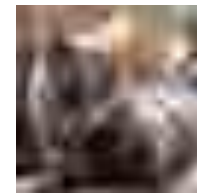
airplane

Alexnet

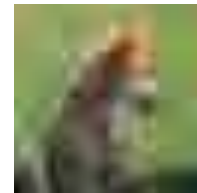
(1,387,786 parameters)



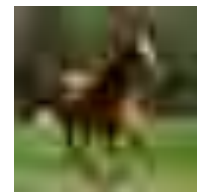
← ?



← ?



← ?



← ?

Train accuracy:



Test accuracy:



Chiyuan Zhang, Samy Bengio, Moritz Hardt, Benjamin Recht, Oriol Vinyals. Understanding deep learning requires rethinking generalization. ICLR 2017

Goal and Challenges

- Explain the excellent generalization of DNNs
- Are DNNs memorizing or generalizing?
- Are DNNs “just” good kNNs?
- **Contributions**
 - DNNs are kNNs in a learned feature space
 - DNNs both memorize and generalize
 - *Memorize* the training set and *generalize* via kNN
 - DNNs might be Bayesian optimal

Experimental Study

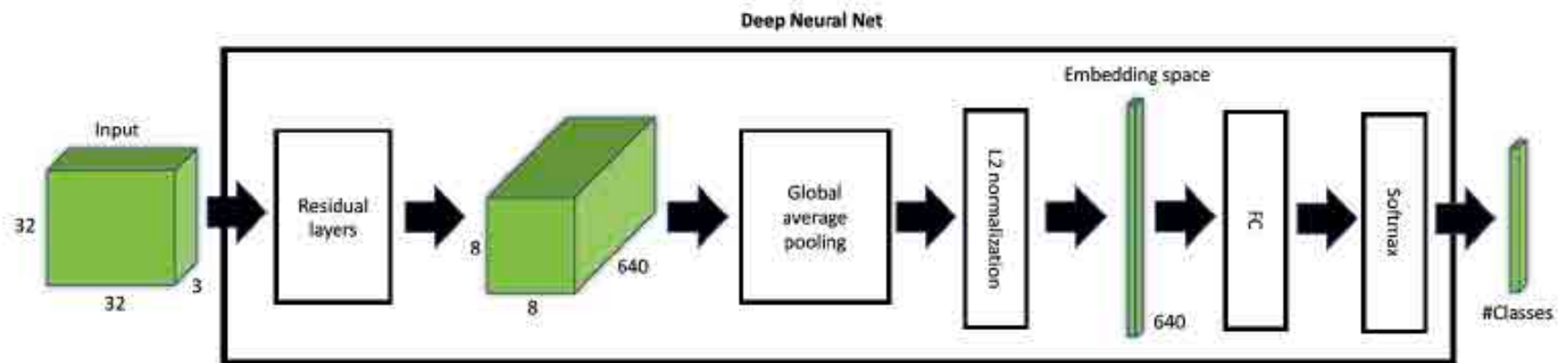
- CIFAR 10/100 and MNIST
- Wide-Resnet 28-10, LeNet, multilayer perception (MLP)

$$MC \triangleq p(f_{kNN}(s) = l | f_{DNN}(s) = l),$$

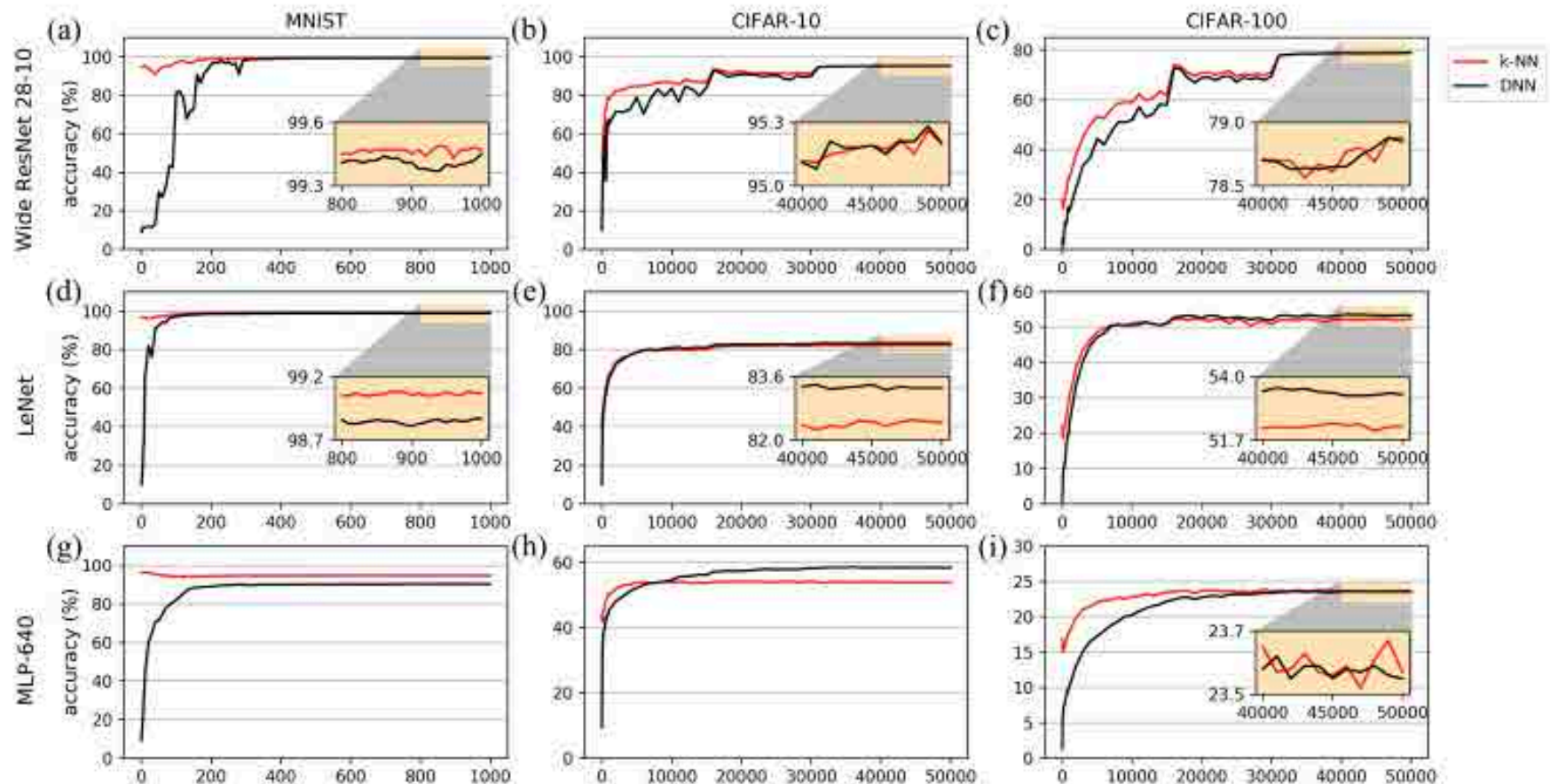
$$ME \triangleq p(f_{kNN}(s) = f_{DNN}(s) | f_{DNN}(s) \neq l),$$

$$\begin{aligned} P_{SAME} &\triangleq p(f_{kNN}(s) = f_{DNN}(s)) \\ &= p(f_{kNN}(s) = l | f_{DNN}(s) = l) p(f_{DNN}(s) = l) \\ &\quad + p(f_{kNN}(s) = f_{DNN}(s) | f_{DNN}(s) \neq l) p(f_{DNN}(s) \neq l) \\ &= MC \times acc + ME \times (1 - acc). \end{aligned}$$

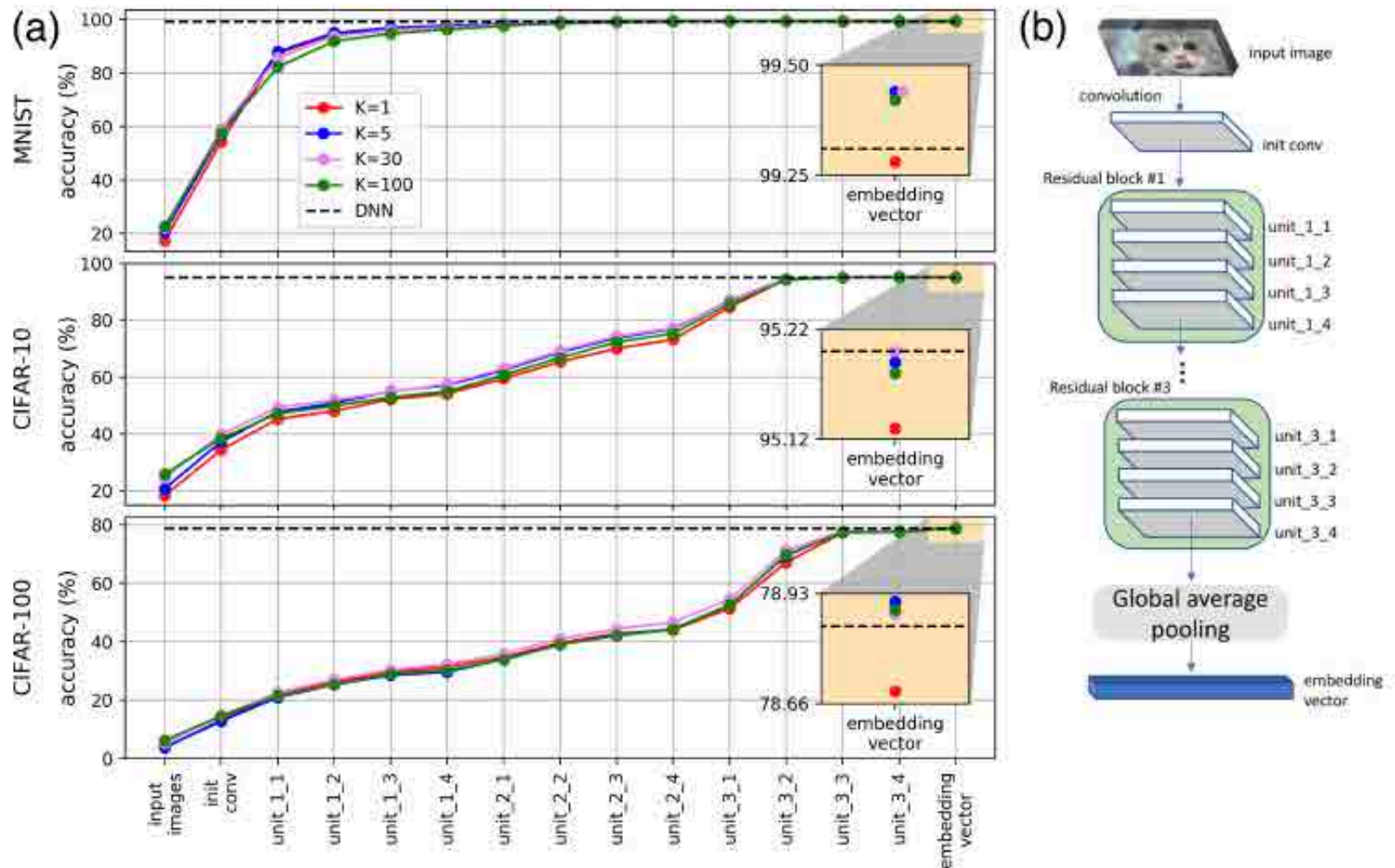
Experimental Study (cont.)



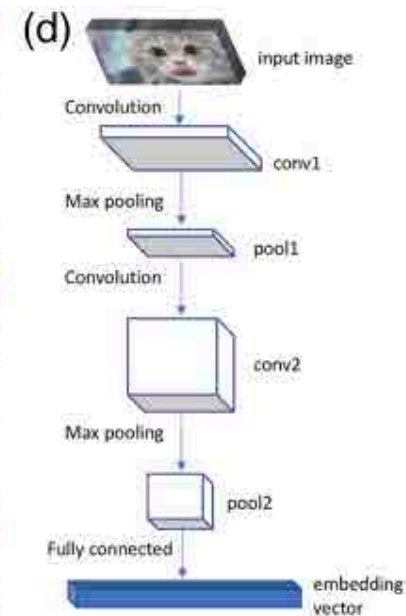
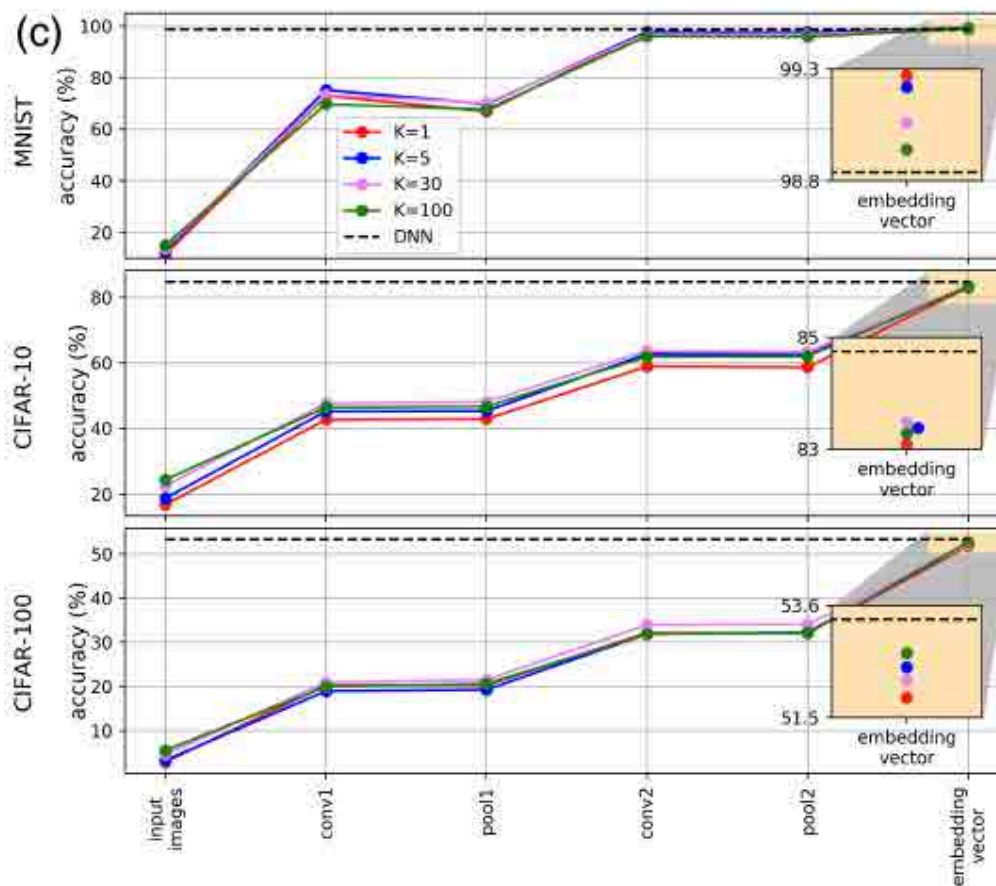
Accuracy as a Function of Training Step



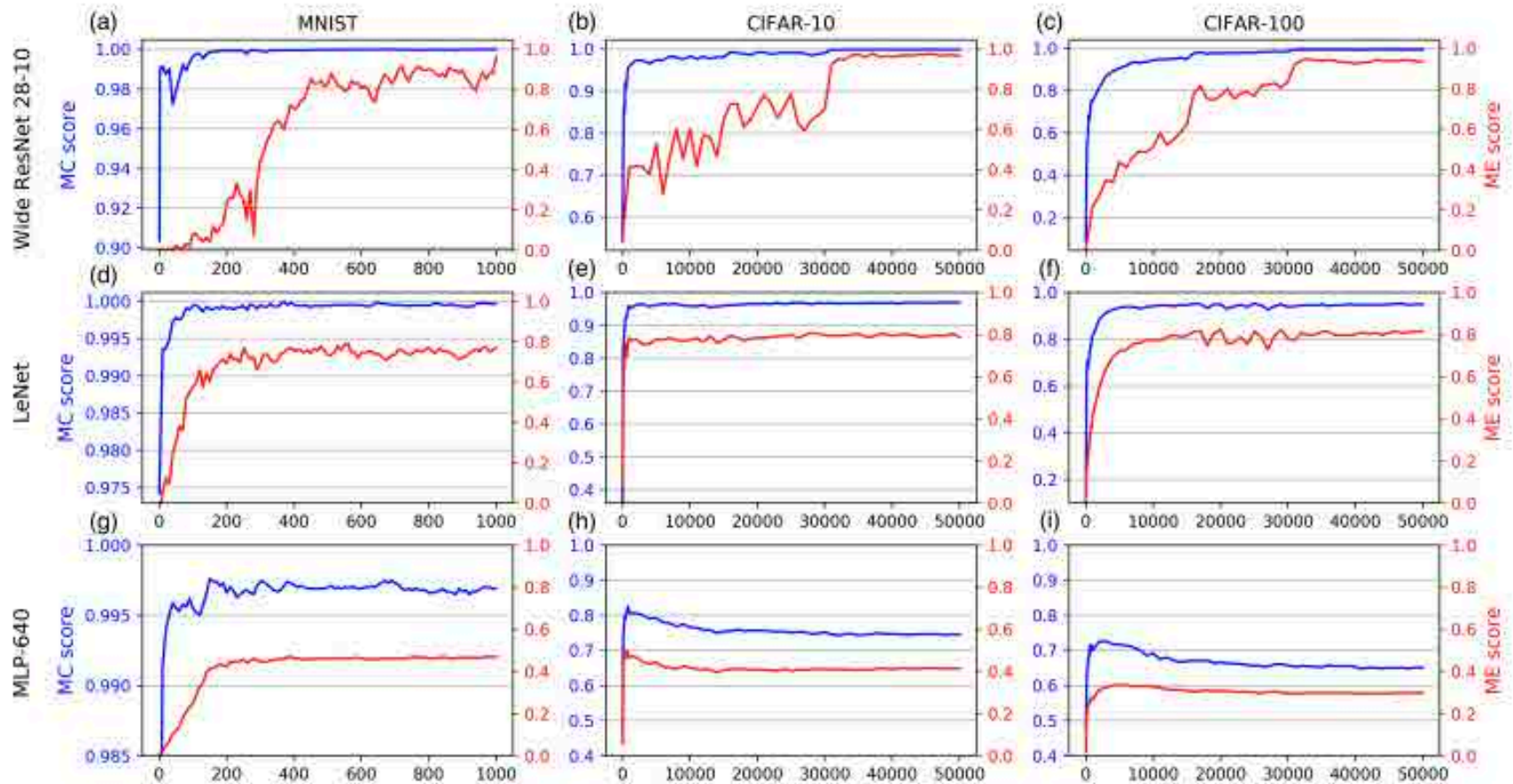
Accuracy as a Function of Layer



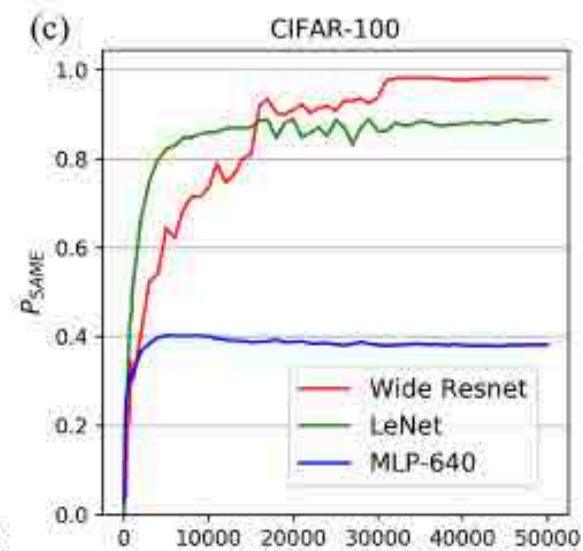
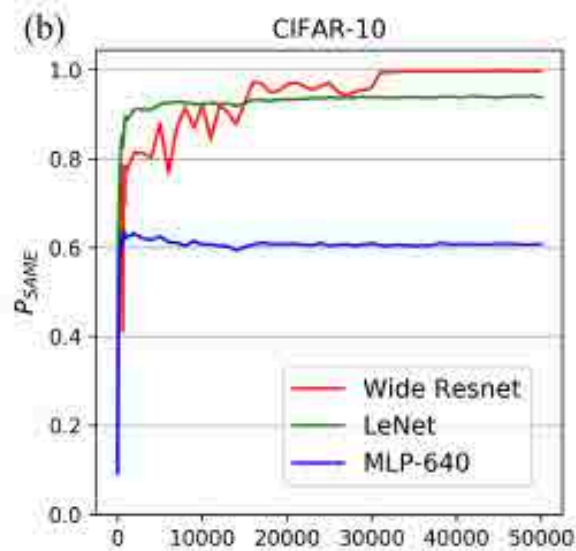
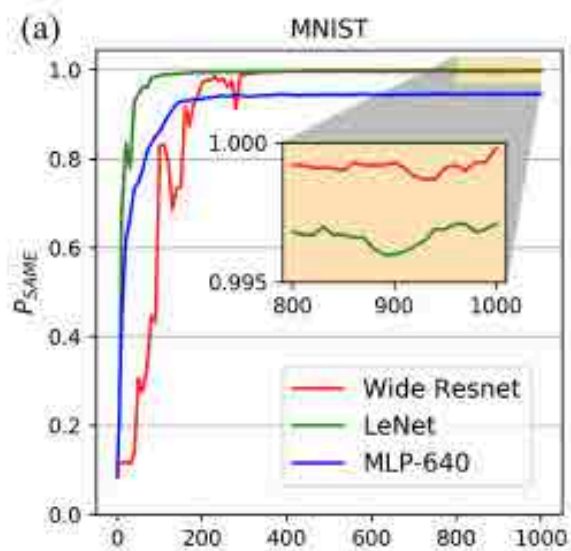
Accuracy as a Function of Layer



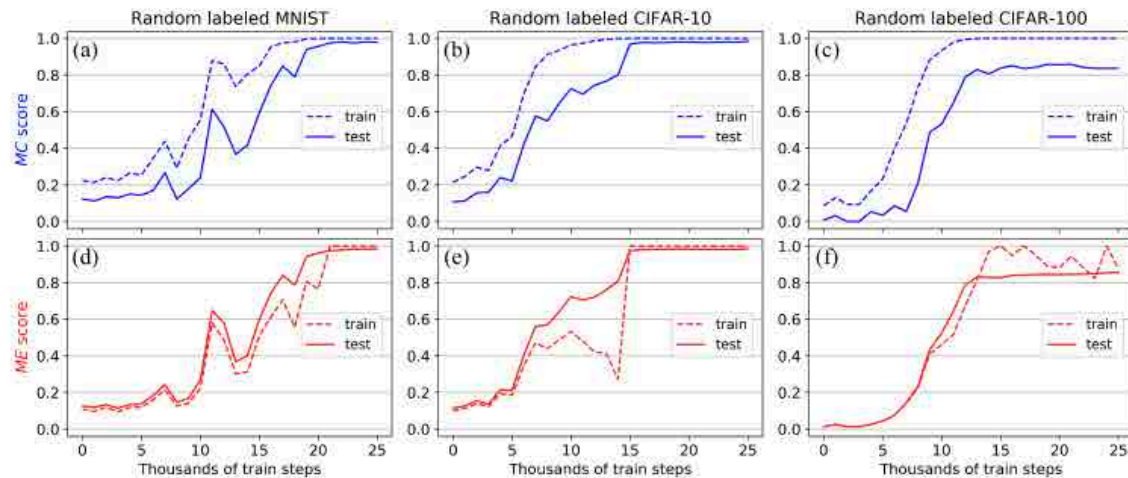
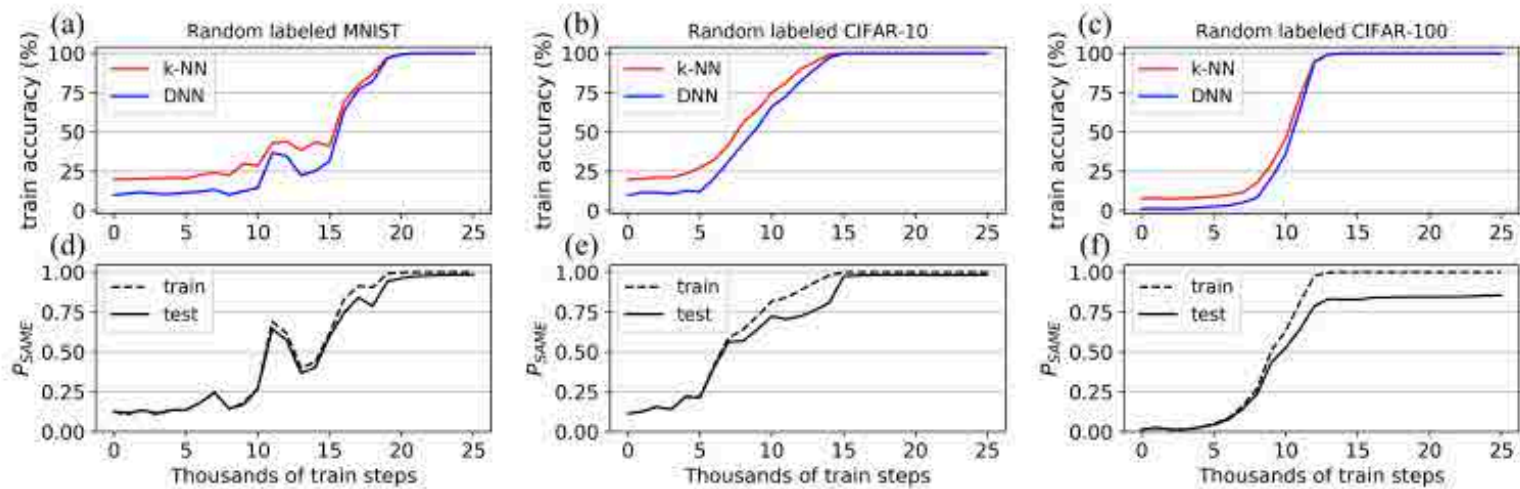
MC and ME



P_{SAME}



Training Performance on Random Labels



Discussion

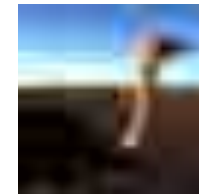
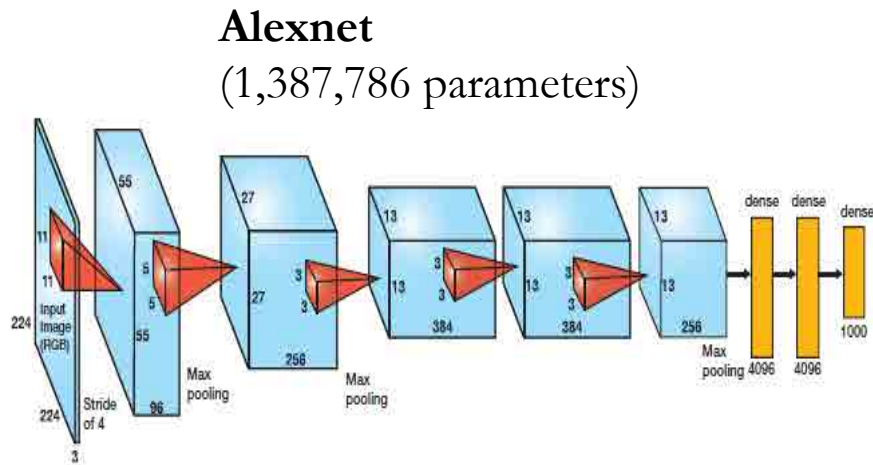
- DNN and kNN are “scary” similar
- DNNs both memorize and generalize
- kNN approach Bayes optimum

$$E^* \leq E \leq E^* \left(2 - \frac{ME^*}{M-1} \right)$$

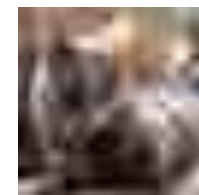
□ Is DNN Bayes optimum?

Regularized Deep Learning with Geometry and Structures

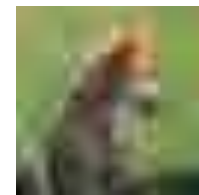
Object Recognition using Deep Learning



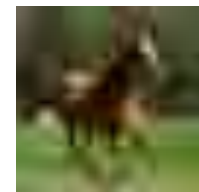
← bird



← cat



← dog



← horse

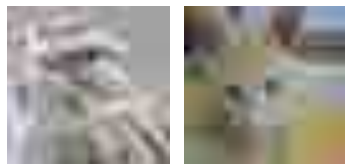
Train accuracy: 99.90%

Test accuracy: 81.22%

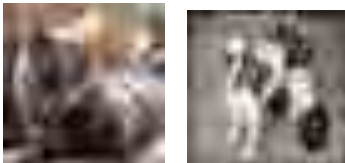
Object Recognition using Deep Learning



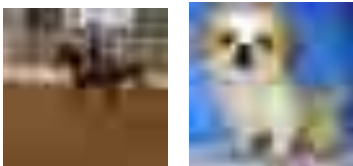
bird horse



airplane dog

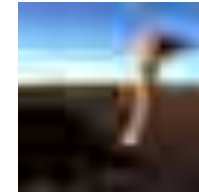
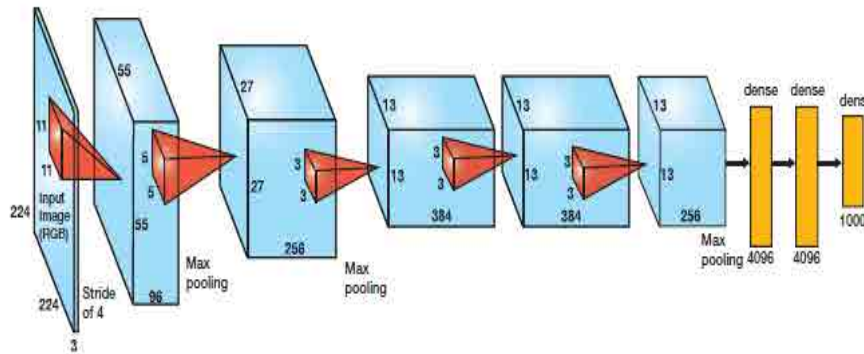


bird cat

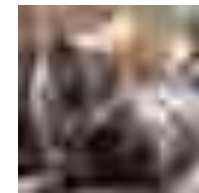


dog airplane

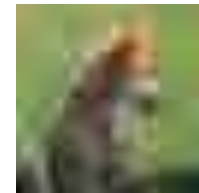
Alexnet
(1,387,786 parameters)



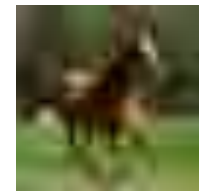
← ?



← ?



← ?

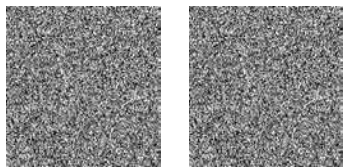


← ?

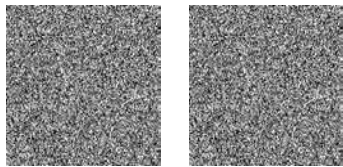
Train accuracy: 99.82%

Test accuracy: 9.86%

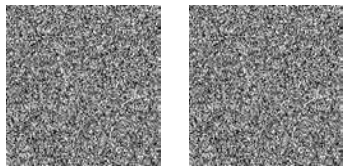
Object Recognition using Deep Learning



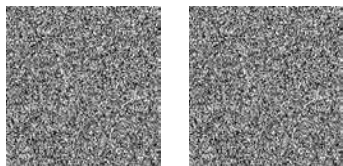
bird horse



airplane dog



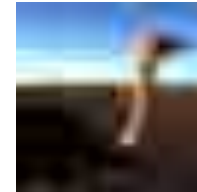
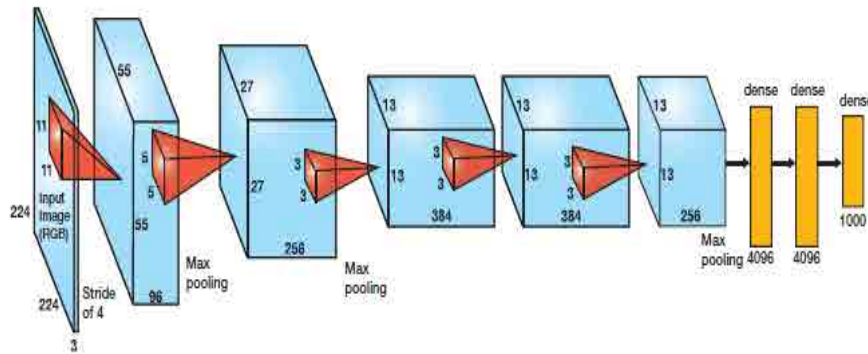
bird cat



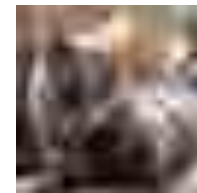
dog airplane

Alexnet

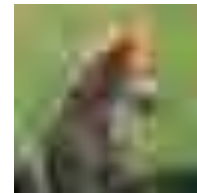
(1,387,786 parameters)



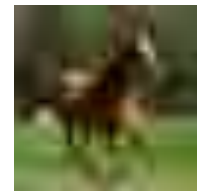
← ?



← ?



← ?



← ?

Train accuracy:



Test accuracy:



Chiyuan Zhang, Samy Bengio, Moritz Hardt, Benjamin Recht, Oriol Vinyals. Understanding deep learning requires rethinking generalization. International Conference on Learning Representations (ICLR), Best Paper Award, 2017

Regularizing Deep Learning

Regularizing with data geometry:

- ❑ Low-rank subspace.
- ❑ Low-dimensional manifold.

Regularizing with structures imposed over and across convolutional filters.

Regularizing with Data Geometry

Low-rank Subspace

9D linear subspace

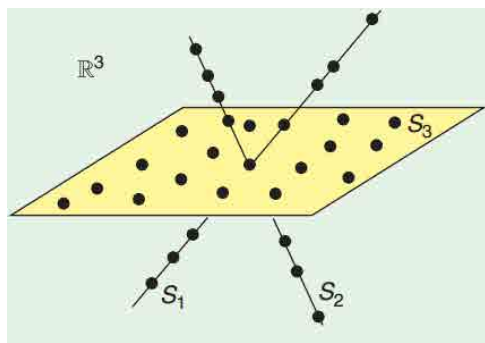
R. Basri and D. W. Jacobs, "Lambertian reflectance and linear subspaces," in IEEE Transactions on Pattern Analysis and Machine Intelligence, vol. 25, no. 2, pp. 218-233, Feb 2003.



$$Y = [Y_1 \ Y_2 \ Y_3]$$

Orthogonal Low-rank Transform

$$\arg \min_{\mathbf{T}} \sum_{c=1}^C \|\mathbf{T}Y_c\|_* - \|\mathbf{T}Y\|_*$$



$\|\mathbf{X}\|_*$ denotes the nuclear norm of the matrix \mathbf{X} :

- The sum of the singular values of \mathbf{A} .
- A good approximation to the matrix rank.

Qiang Qiu, Guillermo Sapiro, "Learning Transformations for Clustering and Classification", Journal of Machine Learning Research (JMLR), 16(Feb):187–225, 2015.

Orthogonal Low-rank Transform

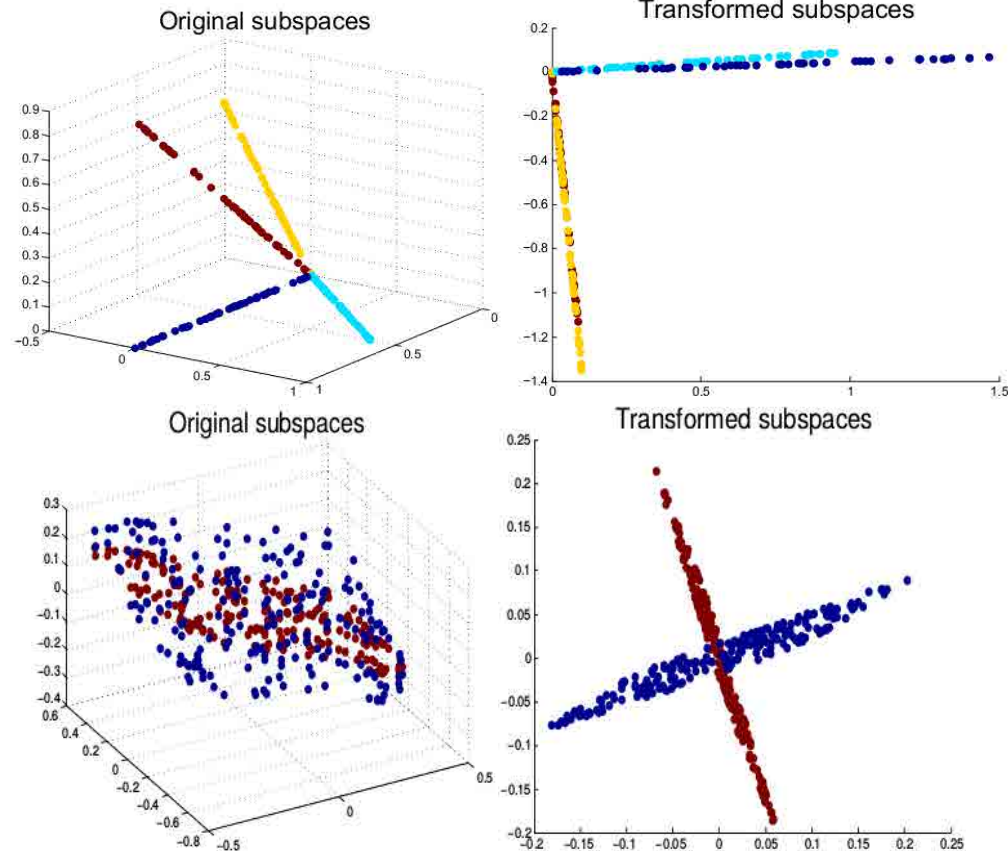
$$\arg \min_{\mathbf{T}} \sum_{c=1}^C \|\mathbf{T}\mathbf{Y}_c\|_* - \|\mathbf{T}\mathbf{Y}\|_*$$

Theorem

$\|[\mathbf{A}, \mathbf{B}]\|_* \leq \|\mathbf{A}\|_* + \|\mathbf{B}\|_*$, equality is satisfied iff \mathbf{A} and \mathbf{B} are orthogonal.

Simultaneously

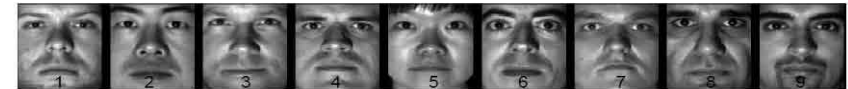
- reduces intra-class variance
- maximize inter-class margin



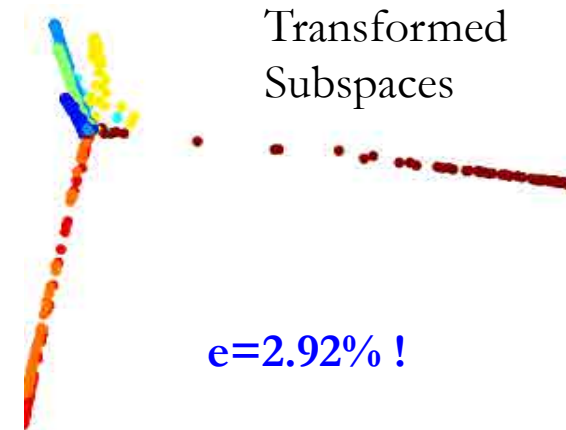
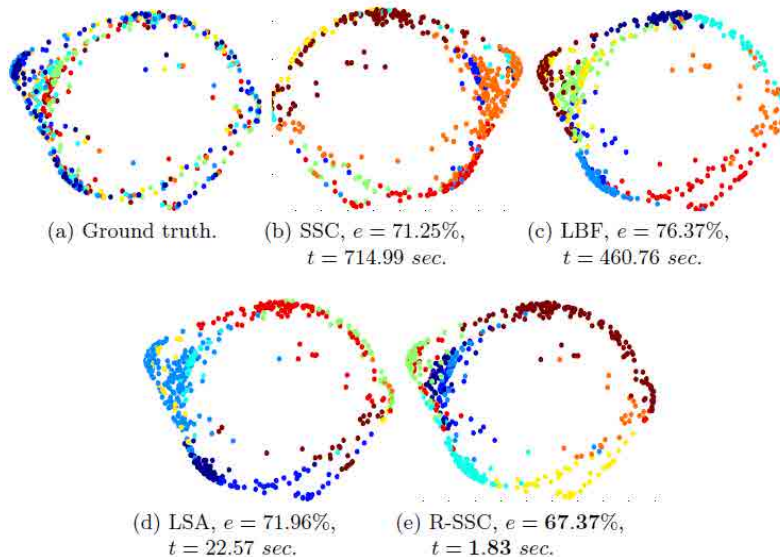
Face Clustering



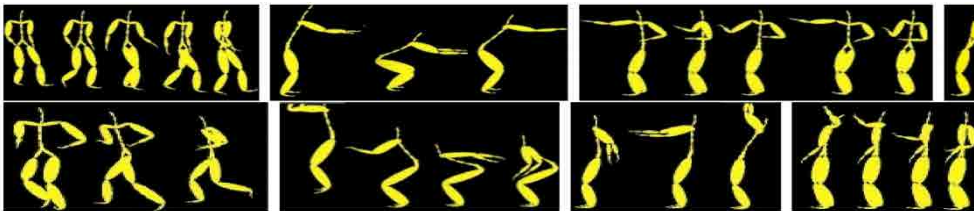
(a) Example illumination conditions.



(b) Example subjects.



Motion Segmentation

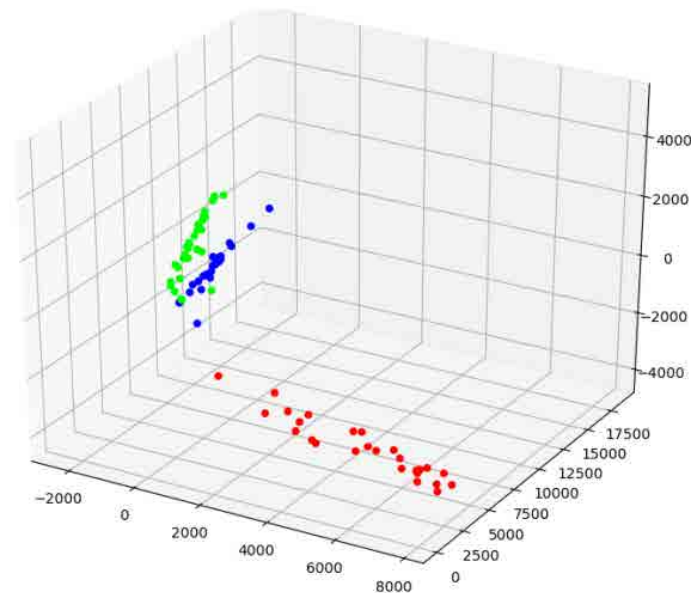
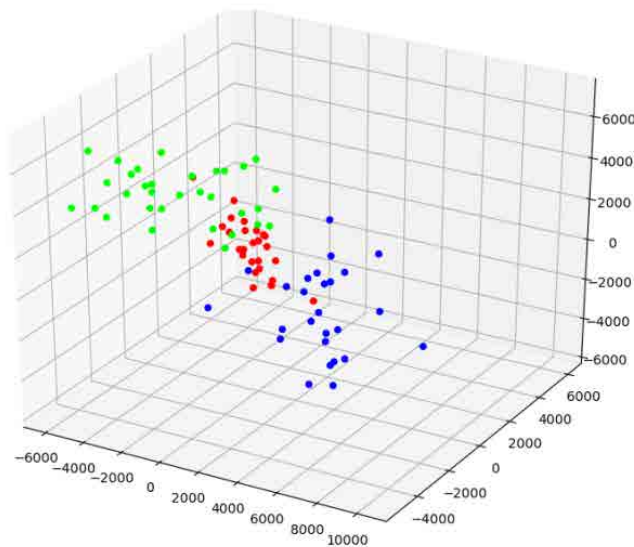
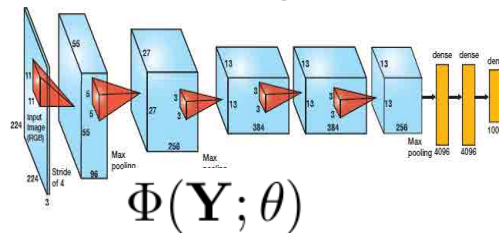


Method	Misclassification (%)
SSC [6]	21.8693
LSA [27]	17.8766
LBF [28]	33.8475
R-SSC	19.0653
R-SSC+RSC	3.902

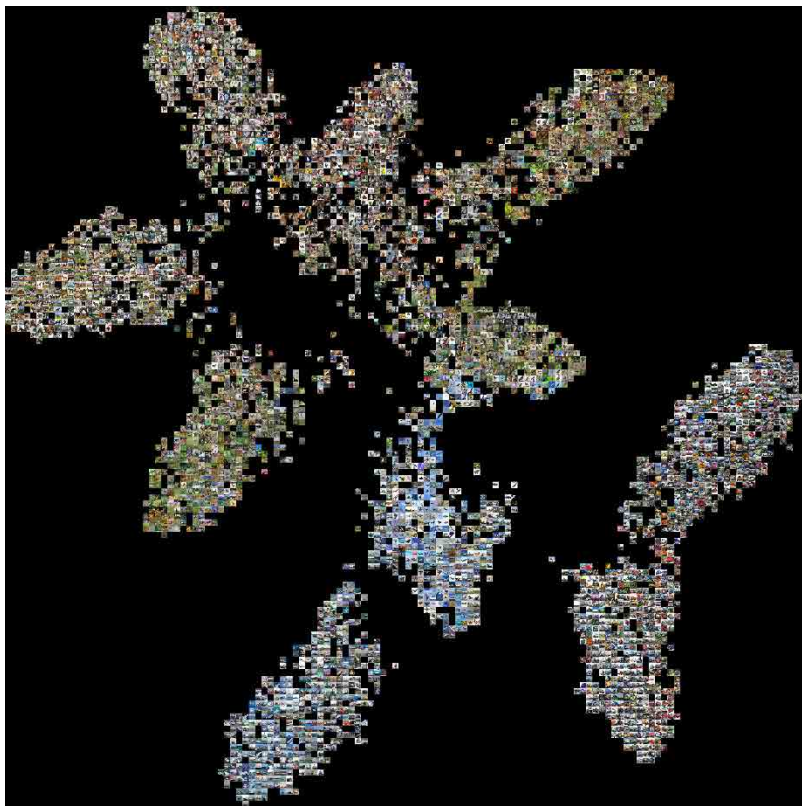
Orthogonal Low-rank Loss

$$\sum_{c=1}^C ||\mathbf{T}\mathbf{Y}_c||_* - ||\mathbf{T}\mathbf{Y}||_* \quad \longrightarrow \quad \sum_{c=1}^C ||\Phi(\mathbf{Y}_c; \theta)||_* - ||\Phi(\mathbf{Y}; \theta)||_*$$

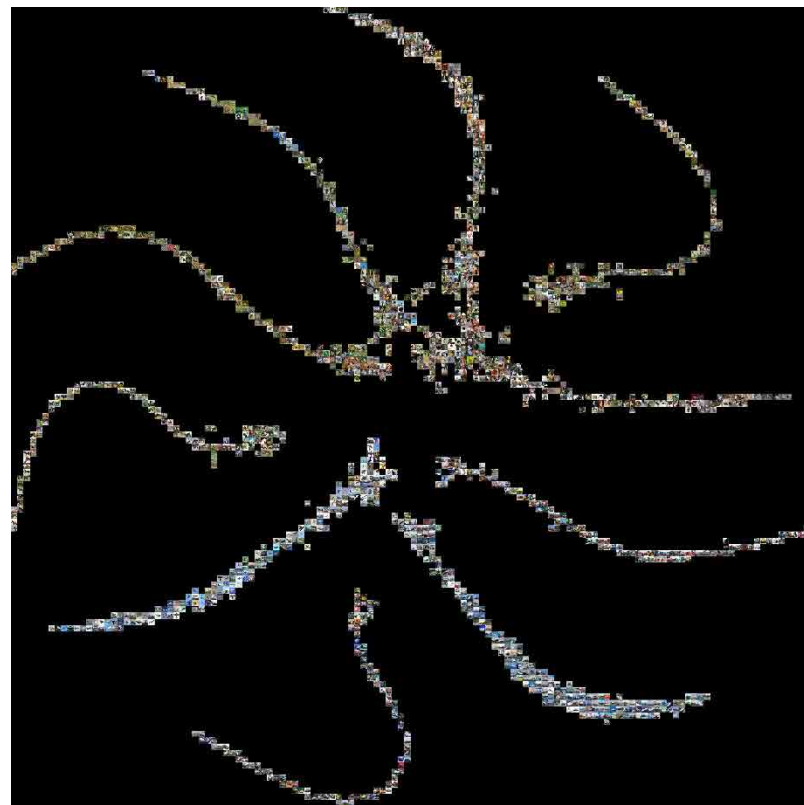
$\mathbf{T} \Rightarrow$



Orthogonal Low-rank Loss



Softmax

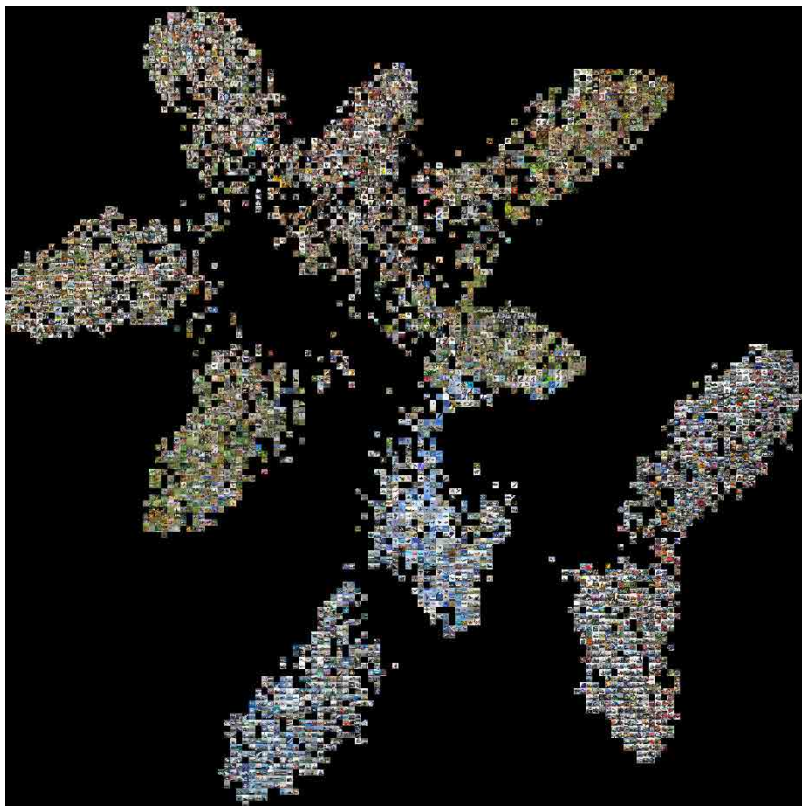


Low-rank

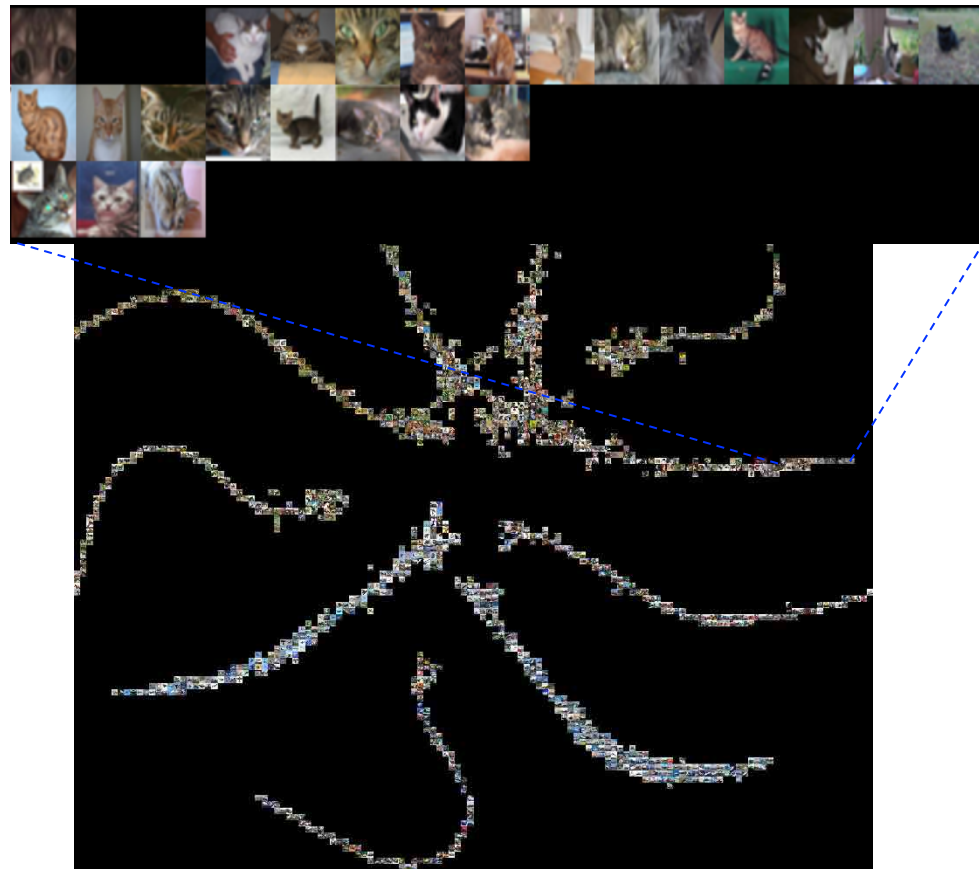
José Lezama, Qiang Qiu, Pablo Musé, Guillermo Sapiro, "OLÉ: Orthogonal Low-rank Embedding, A Plug and Play Geometric Loss for Deep Learning", Computer Vision and Patt. Recn. (CVPR), 2018 26

<https://github.com/jlezama/OrthogonalLowrankEmbedding>

Orthogonal Low-rank Loss



Softmax



Low-rank

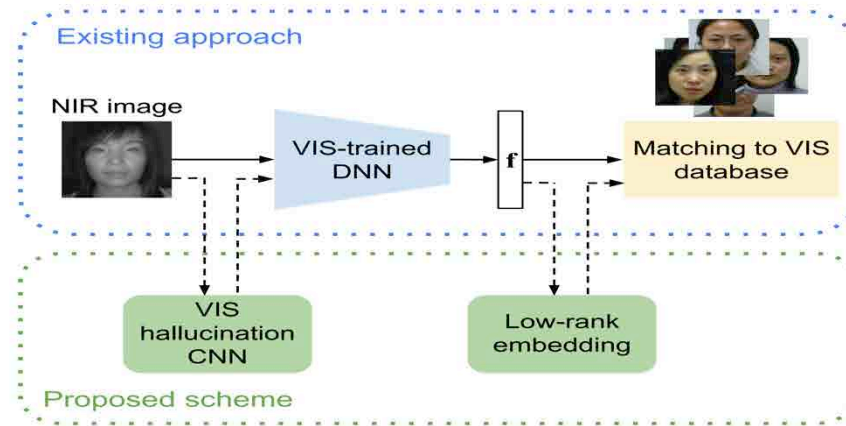
José Lezama, Qiang Qiu, Pablo Musé, Guillermo Sapiro, "OLÉ: Orthogonal Low-rank Embedding, A Plug and Play Geometric Loss for Deep Learning", Computer Vision and Patt. Recn. (CVPR), 2018 27

<https://github.com/jlezama/OrthogonalLowrankEmbedding>

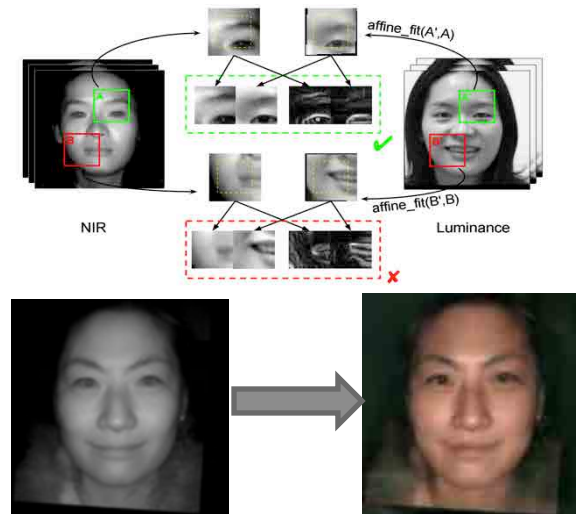
Orthogonal Low-rank Loss

Dataset	Architecture	λ	% Error ($L_o + \lambda \cdot L_s$)	% Error (L_s only)
SVHN	DenseNet-40-12 [11]	1/2	3.62 \pm 0.04	3.93 \pm 0.08
MNIST	DenseNet-40-12	1/2	0.78 \pm 0.04	0.88 \pm 0.03
CIFAR10+	DenseNet-40-12	1/8	5.30 \pm 0.26	5.54 \pm 0.13
CIFAR10+	ResNet-110 [8]	1/4	5.39 \pm 0.25	6.05 \pm 0.8
CIFAR10+	VGG-19 [29]	1/4	7.13 \pm 0.2	7.37 \pm 0.11
CIFAR10+	VGG-11	1/2	7.73 \pm 0.14	8.06 \pm 0.22
CIFAR10	VGG-16 [18]	1/2	7.22 \pm 0.14	8.23 \pm 0.13
CIFAR100+	PreResNet-110 [9]	1/20	22.8 \pm 0.34	23.01 \pm 0.19
CIFAR100+	VGG-19	1/10	27.54 \pm 0.11	28.04 \pm 0.42
CIFAR100	VGG-19	1/10	37.25 \pm 0.33	38.15 \pm 0.28
FaceScrub-500	VGG-FACE [22]	1/10	1.55 \pm 0.02	2.49 \pm 0.01
STL-10	CNN-5	1/16	25.42 \pm 0.20	28.68 \pm 0.67
STL-10+	CNN-5	1/4	16.68 \pm 0.24	18.22 \pm 0.27

Cross-spectral Face Recognition

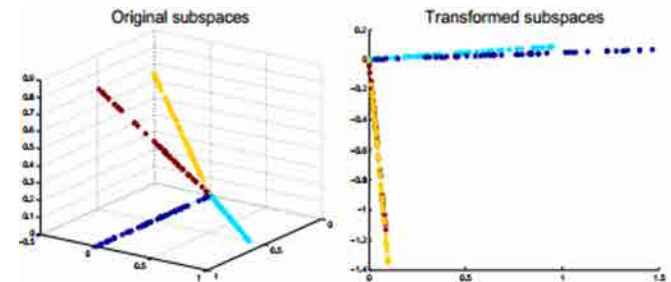


NIR-VIS Hallucination



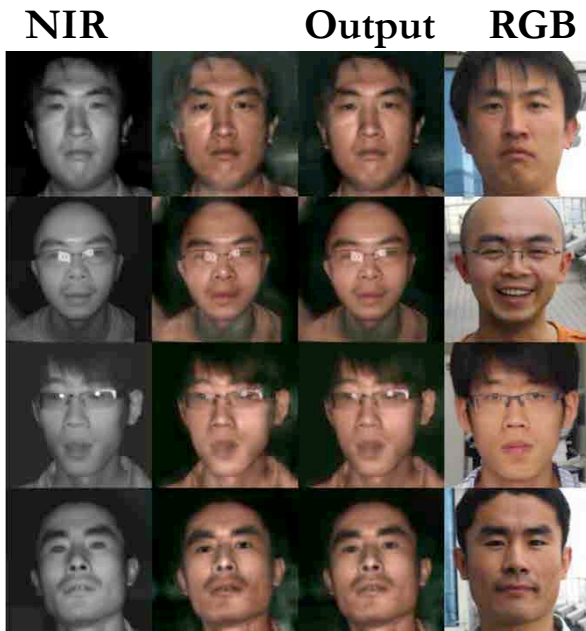
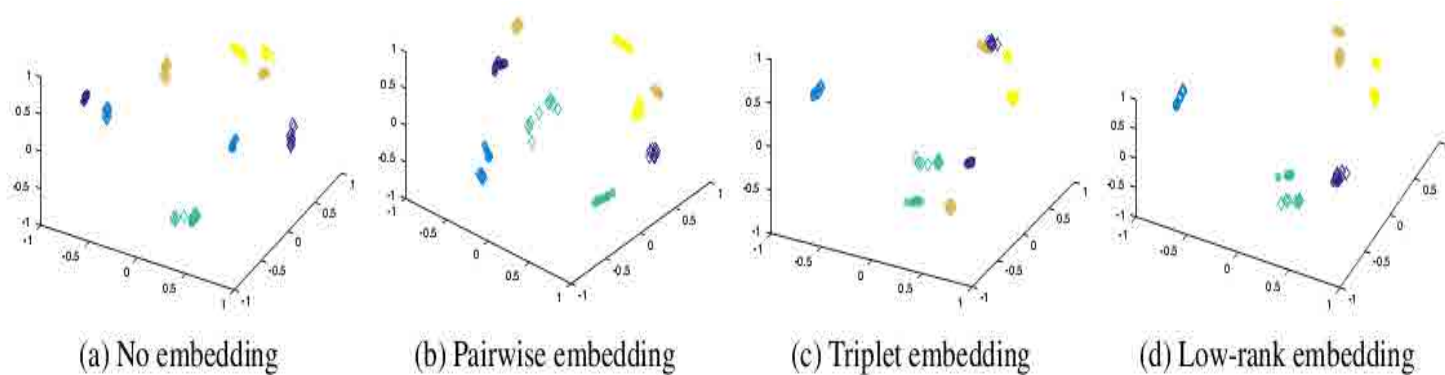
Low-rank Embedding

$$\sum_{c=1}^C ||\mathbf{T}\mathbf{Y}_c||_* - ||\mathbf{T}\mathbf{Y}||_*$$



Jose Lezama, Qiang Qiu, Guillermo Sapiro, "Not Afraid of the Dark: NIR-VIS Face Recognition via Cross-spectral Hallucination and Low-rank Embedding", Computer Vision and Patt. Recn. (CVPR), 2017

Cross-spectral Face Recognition



	Accuracy (%)
VGG-S	75.04
VGG-S + Hallucination	80.65
VGG-S + Low-rank	89.88
VGG-S + Hallucination + Low-rank	95.72
VGG-face	72.54
VGG-face + Hallucination	83.10
VGG-face + Low-rank	82.26
VGG-face + Hallucination + Low-rank	91.01
COTS	83.84
COTS + Hallucination	93.02
COTS + Low-rank	91.83
COTS + Hallucination + Low-rank	96.41

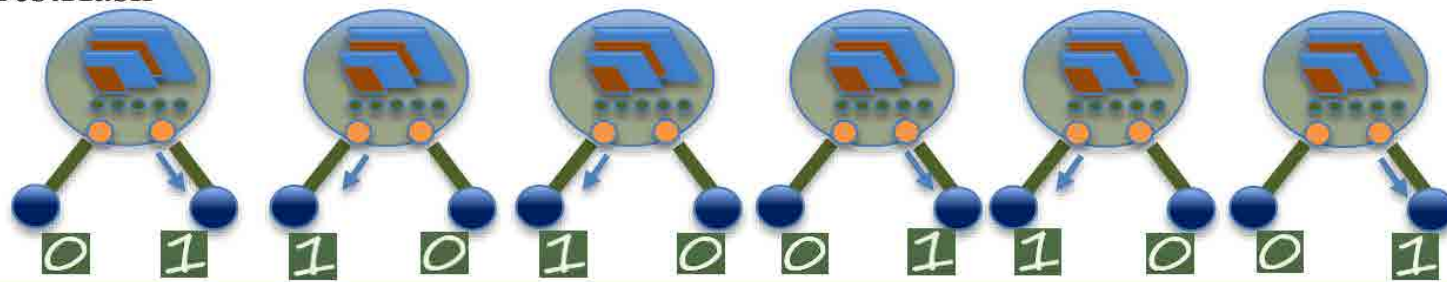
Jose Lezama, Qiang Qiu, Guillermo Sapiro, "Not Afraid of the Dark: NIR-VIS Face Recognition via Cross-spectral Hallucination and Low-rank Embedding", Computer Vision and Patt. Recn. (CVPR), 30 2017

Image Hashing

Each face is represented by a 48-bit hash code.



ForestHash



We set '1' for the visited nodes, and '0' for the rest, obtaining a $(2^d - 2)$ -bit hash code.

- Random class grouping (uniqueness)
- Orthogonal Low-rank loss (consistency)
- Near-optimal Code aggregation

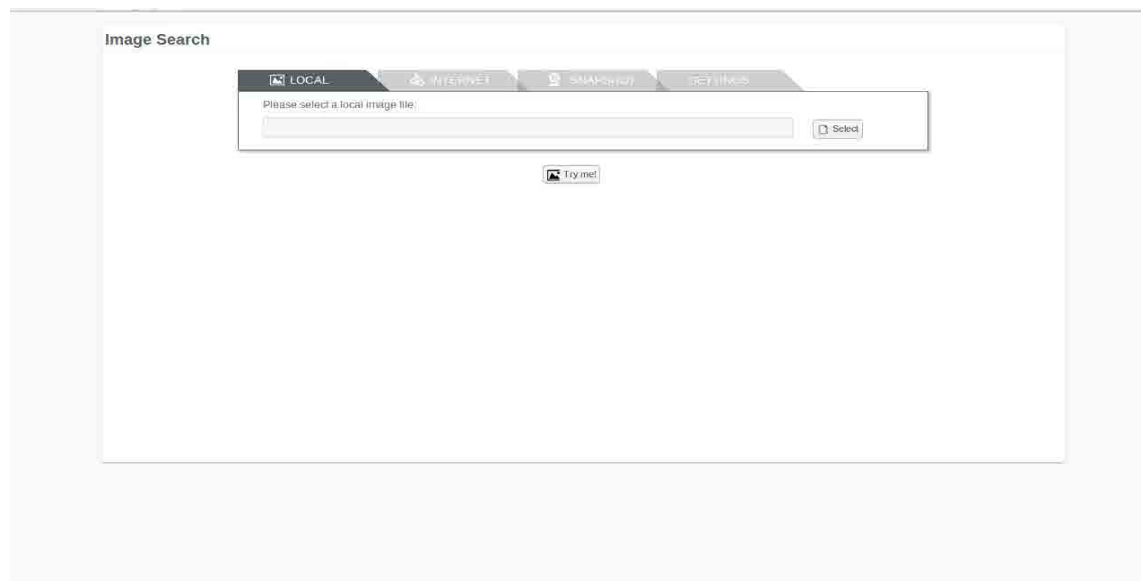
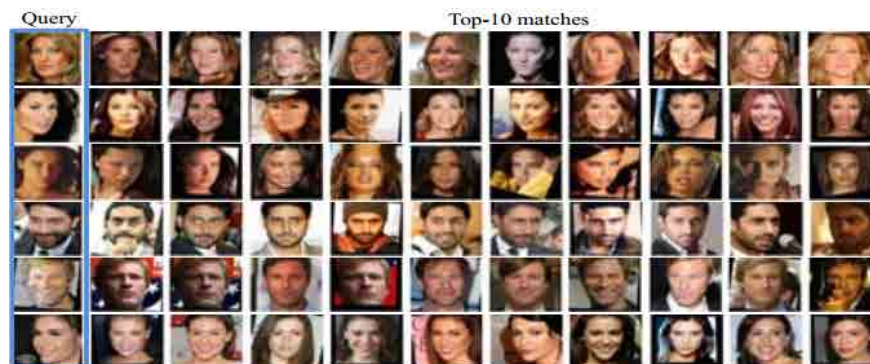
CNN2		
1	Conv+ReLU+MaxPool	$5 \times 5 \times 3 \times 64$
2	Conv+ReLU+MaxPool	$5 \times 5 \times 64 \times 32$
3	FC	output: 256

Train and deploy in parallel!!

Image Hashing

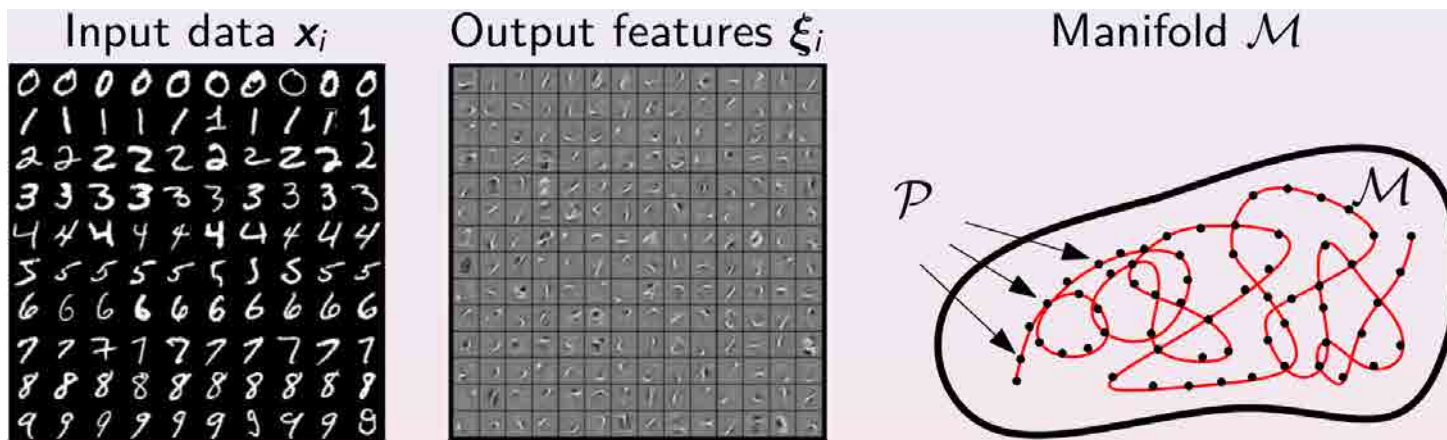
Method	radius = 0			radius ≤ 2		
	Precision	Recall	F1	Precision	Recall	F1
KLSH (36-bit) [15]	16.97	3.73	6.11	31.93	8.38	13.28
AGH1 (36-bit) [19]	18.38	56.12	27.69	7.75	82.30	14.16
AGH2 (36-bit) [19]	13.56	57.48	21.94	5.53	89.52	10.41
LDAHash (36-bit) [64]	23.42	0.65	1.26	45.11	10.25	16.71
Proposed (36-bit)	82.17	82.29	82.23	47.58	89.38	62.10
Proposed (48-bit)	90.74	80.42	85.27	81.74	87.41	84.48

~30 microseconds to index a face.
~20 milliseconds to scan one million faces.



Live Demo over 5M faces.

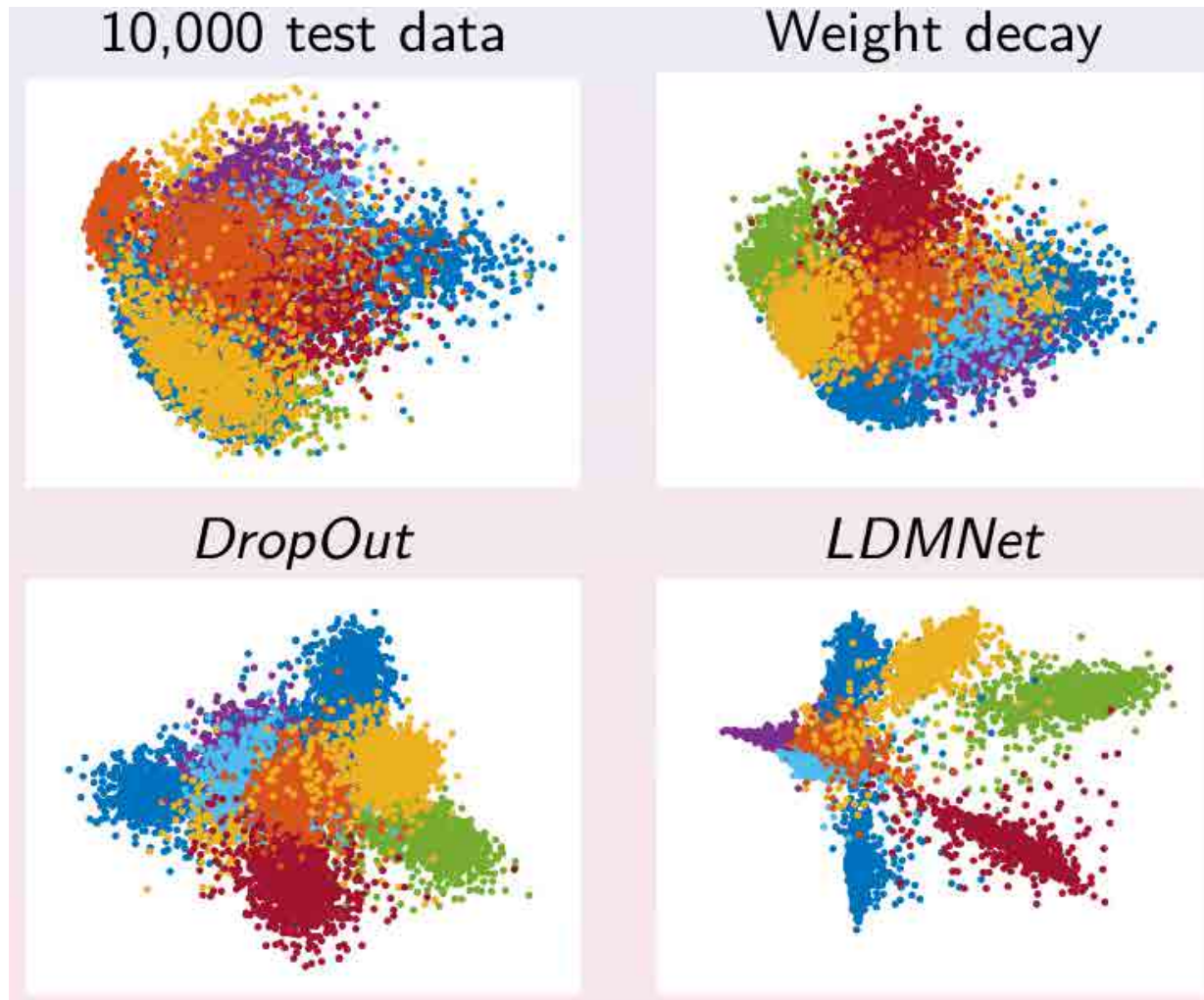
Low-dimensional Manifold



< 56 dimensions

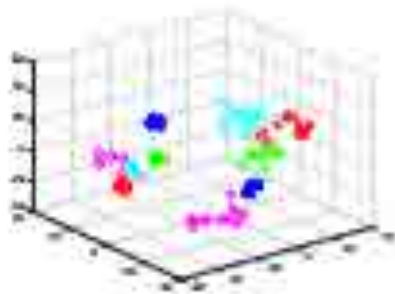
$$\begin{aligned} \min_{\theta, \mathcal{M}} \quad & J(\theta) + \frac{\lambda}{|\mathcal{M}|} \int_{\mathcal{M}} \dim(\mathcal{M}(\mathbf{p})) d\mathbf{p} \\ \text{s.t.} \quad & \{(\mathbf{x}_i, f_{\theta}(\mathbf{x}_i))\}_{i=1}^N \subset \mathcal{M}, \end{aligned}$$

Low-dimensional Manifold

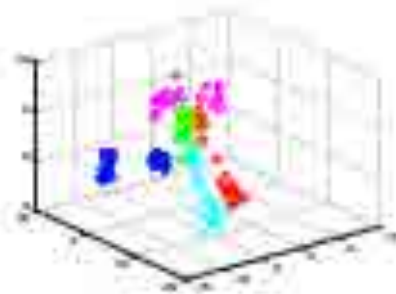


Wei Zhu, Qiang Qiu, Jiaji Huang, Robert Calderbank, Guillermo Sapiro, Ingrid Daubechies, "LDMNet: Low Dimensional Manifold Regularized Neural Networks", Computer Vision and Patt. Recn. (CVPR), 2018

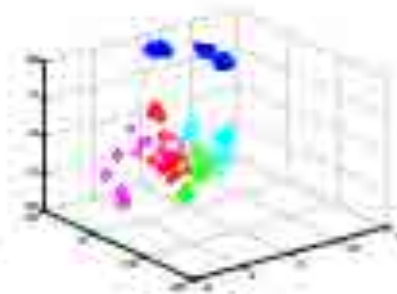
Low-dimensional Manifold



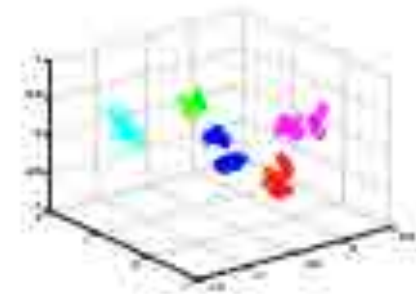
(a) VGG-face



(b) Weight decay



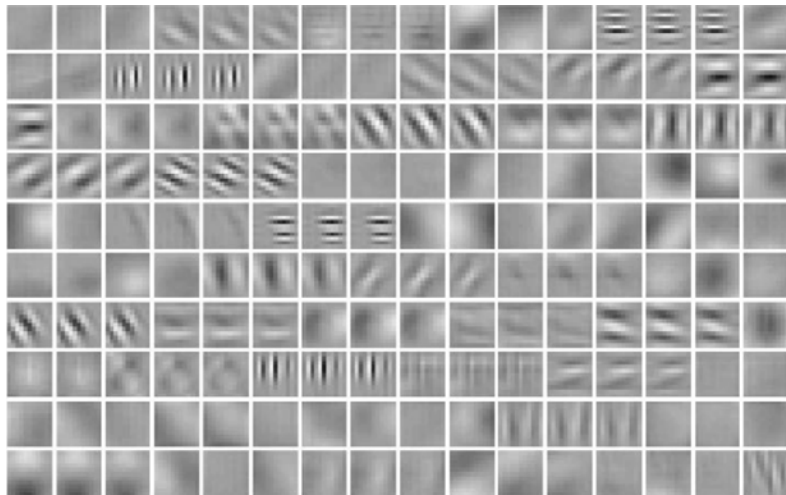
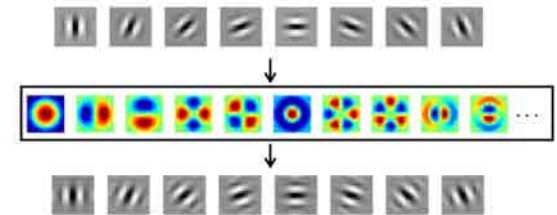
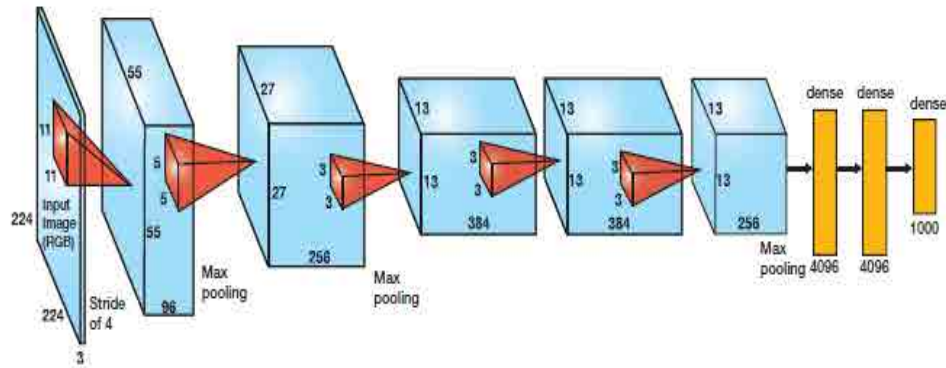
(c) DropOut



(d) LDMNet

Regularizing with Filter Structures

Decompose Filters over Bases

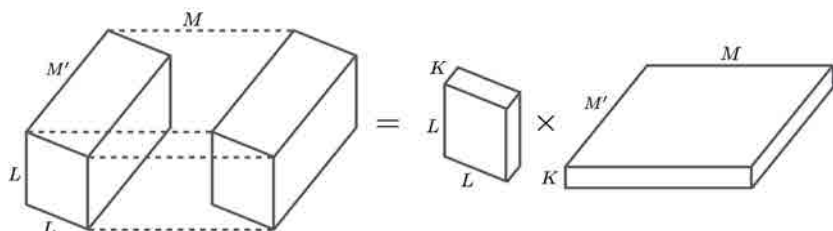


$$\text{Filter} = a \cdot \text{Base 1} + b \cdot \text{Base 2} + c \cdot \text{Base 3} + \dots$$

The equation shows a single grayscale filter on the left, followed by an equals sign, then a coefficient 'a' multiplied by a red circular heatmap (Base 1), plus a coefficient 'b' multiplied by a blue and red horizontal heatmap (Base 2), plus a coefficient 'c' multiplied by a blue and red vertical heatmap (Base 3), followed by an ellipsis '...'.

- Reduce parameters and computations (K/L^2).
- Impose filter regularity by bases truncation.

Decomposed Convolutional Filters

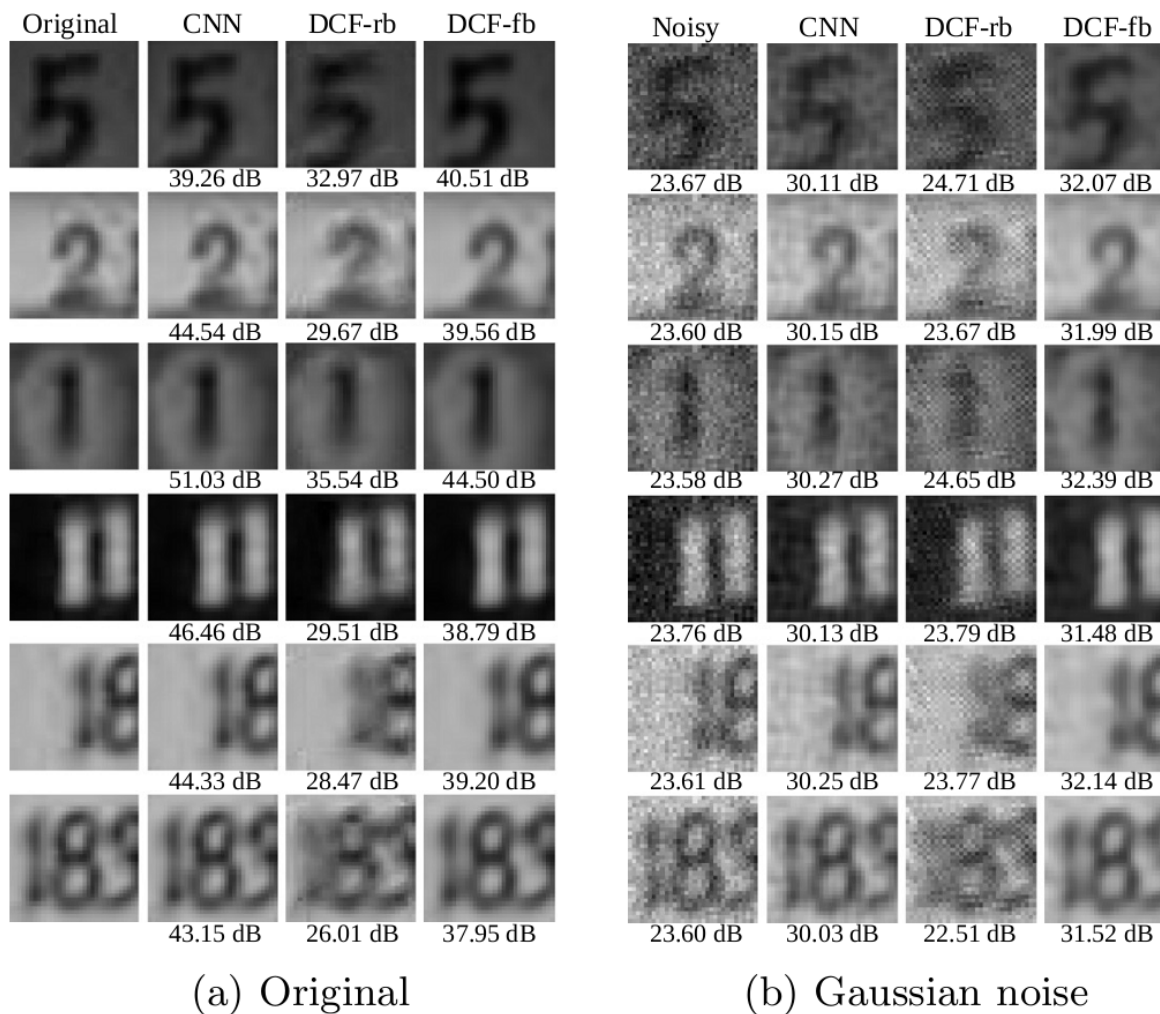


Layer	CNN	DCFNet
1	conv $3 \times 3 \times 3 \times 64$	$3 \times 3 \times 3$ basis conv $1 \times 1 \times 9 \times 64$
2	ReLU	
3	conv $3 \times 3 \times 64 \times 64$	$3 \times 3 \times 3$ basis conv $1 \times 1 \times 192 \times 64$
4-5	ReLU, maxPool 2×2	
6	conv $3 \times 3 \times 64 \times 128$	$3 \times 3 \times 3$ basis conv $1 \times 1 \times 192 \times 128$
7	ReLU	
8	conv $3 \times 3 \times 128 \times 128$	$3 \times 3 \times 3$ basis conv $1 \times 1 \times 384 \times 128$
9-10	ReLU, maxPool 2×2	
(1-31 CNN layers are identical to <i>vgg-face</i> model in [25].)		
32	conv $5 \times 5 \times 512 \times 512$	$8 \times 5 \times 5$ basis conv $1 \times 1 \times 4096 \times 512$
33-34	ReLU, dropout	
35	conv $3 \times 3 \times 512 \times 512$	$3 \times 3 \times 3$ basis conv $1 \times 1 \times 1536 \times 512$
36-39	ReLU, dropout, FC, softmax	

Decomposed Convolutional Filters

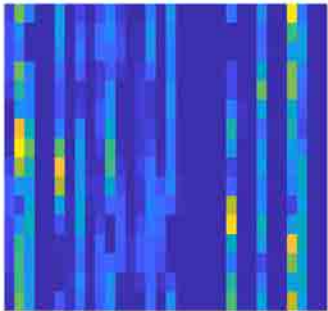
MNIST conv-2, 5x5						
	fb	rb	pca-s	pca-f	# param.	# MFlops
CNN	99.40				2.61×10^4	3.37
$K=14$	99.47	99.35	99.38	99.41	1.46×10^4	2.40
$K=8$	99.48	99.26	99.28	99.45	8.40×10^3	1.37
$K=5$	99.39	99.28	99.28	99.43	5.28×10^3	0.86
$K=3$	99.40	98.69	99.19	99.35	3.20×10^3	0.51
SVHN conv-3, 5x5						
	fb	rb	pca-s	pca-f	# param.	# MFlops
CNN	94.22				1.03×10^6	201.64
$K=14$	94.63	93.75	94.52	94.42	5.74×10^5	121.91
$K=8$	94.39	92.05	93.85	94.30	3.30×10^5	69.67
$K=5$	93.93	91.28	92.34	94.03	2.06×10^5	43.55
$K=3$	92.84	88.47	91.88	93.10	1.24×10^5	26.13
Cifar10 conv-3, 5x5						
	fb	rb	pca-s	pca-f	# param.	# MFlops
CNN	85.66				(same as above)	
$K=14$	85.88	84.76	85.27	85.34		
$K=8$	85.30	81.27	84.70	85.09		
$K=5$	84.35	77.96	83.12	83.94		
$K=3$	83.12	74.05	80.94	82.91		
Cifar10 vgg-16, 3x3						
	fb	rb	pca-s	pca-f	# param.	# MFlops
CNN	87.02				1.47×10^7	547.20
$K=5$	87.79	84.16	87.98	87.60	8.18×10^6	311.68
$K=3$	88.21	78.46	87.45	87.54	4.91×10^6	187.02
	Accuracy		# param.		# GFlops	
<i>VGG-face</i>	97.27 %		-		-	
CNN	97.65 %		21.26×10^6		30.05	
DCFNet	97.32 %		7.01×10^6		10.09	

Decomposed Convolutional Filters

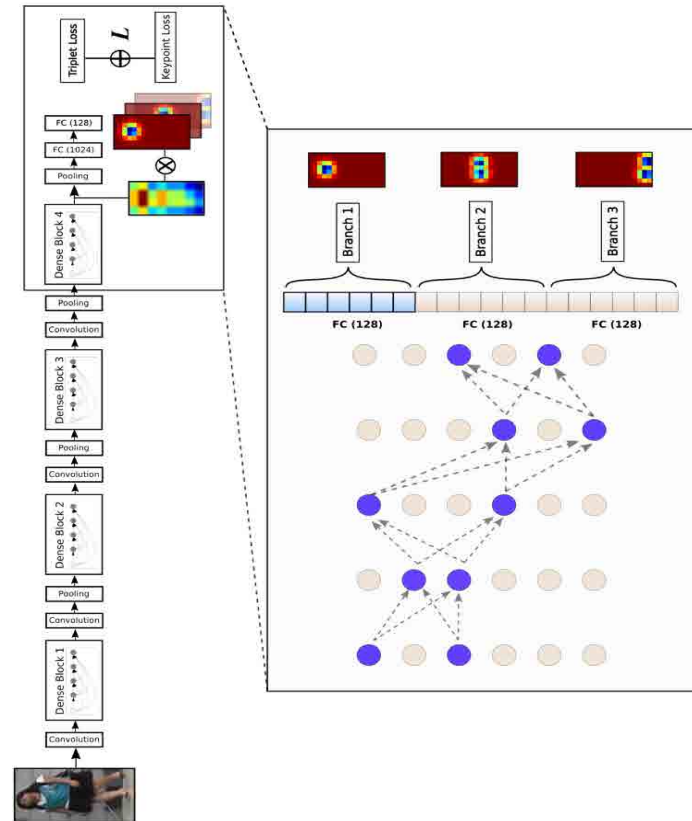


Structures across Filters

Orientation equivariant learning



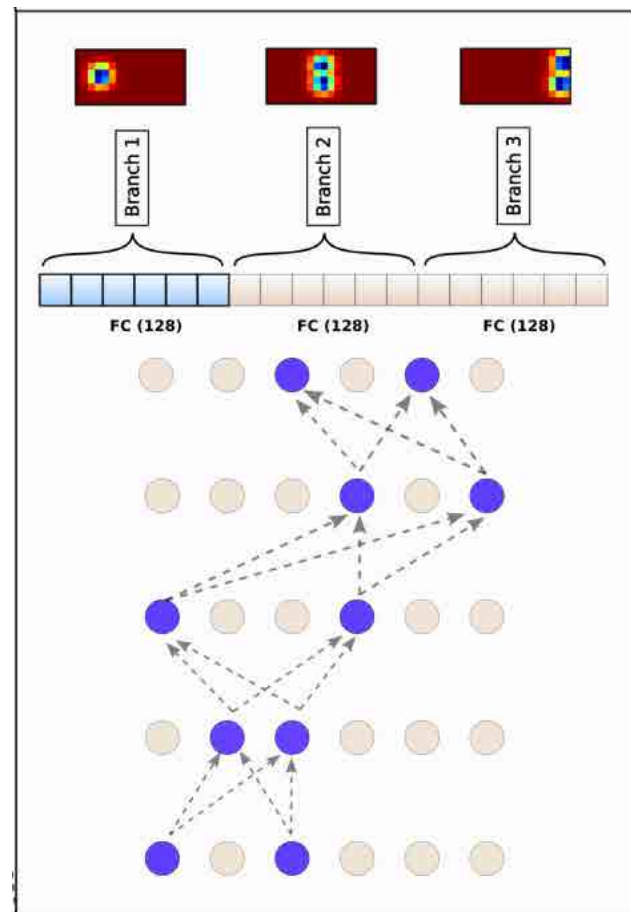
Virtual branching



Person Re-Identification



1. Nose
2. Neck
3. Right Shoulder
4. Right Elbow
5. Right Wrist
6. Left Shoulder
7. Left Elbow
8. Left Wrist
9. Right Hip
10. Right Knee
11. Right Ankle
12. Left Hip
13. Left Knee
14. Left Ankle
15. Right Eye
16. Left Eye
17. Right Ear
18. Left Ear



Albert Gong, Qiang Qiu, Guillermo Sapiro, "Virtual CNN Branching: Efficient Feature Ensemble for Person Re-Identification", arXiv:1803.05872, 2018 (High school research)

Person Re-Identification

	Single Query			Multi-query		
Method	mAP	Rank-1	Rank-5	mAP	Rank-1	Rank-5
Gated Siamese CNN [34]	39.95	65.88	-	48.45	76.04	-
PIE [3]	53.87	78.65	90.26	-	-	-
JLML [22]	65.5	85.1	-	74.5	89.7	-
PAN [3]	63.35	82.81	-	71.72	88.18	-
Res50 + Attribute [21]	64.67	84.29	93.20	-	-	-
GoogLeNet + DTL [20]	65.5	83.7	-	73.08	89.6	-
PDC [4]	63.41	84.14	92.73	-	-	-
SpindleNet [5]	-	76.9	91.5	-	-	-
TriNet [†] [17]	69.14	84.92	94.21	76.42	90.53	96.29
MobileNet + DML [†] [35]	68.86	87.73	-	77.14	91.66	-
Baseline	68.3	83.3	93.1	75.8	90.1	95.9
Human Landmark	70.8	87.9	96.0	79.4	93.5	98.9
Pose Orientation	71.1	87.7	96.5	79.3	93.3	98.5

Market-1501

	Labeled			Detected		
Method	mAP	Rank-1	Rank-5	mAP	Rank-1	Rank-5
Gated Siamese CNN [34]	-	-	-	51.25	61.8	80.9
PIE [3]	-	-	-	67.21	61.50	89.30
JLML [22]	-	83.2	98.0	-	80.6	96.9
PAN [3]	35.03	36.86	56.86	34.00	36.29	55.50
GoogLeNet + DTL [20]	-	85.4	-	-	84.1	-
PDC [4]	-	88.70	-	-	78.29	-
SpindleNet [5]	-	-	-	-	88.5	97.8
TriNet [†] [17]	-	89.63	99.01	-	87.58	98.17
Baseline	93.6	88.2	99.4	92.0	86.4	98.1
Human Landmark	95.5	91.0	99.8	94.7	88.9	99.4
Pose Orientation	95.8	90.9	99.6	94.5	89.3	99.4

CUHK03

Thank you!